ARTICLE

Carbon Nanotube Reinforced Polylactide–Caprolactone Copolymer: Mechanical Strengthening and Interaction with Human Osteoblasts in Vitro

D. Lahiri,[†] F. Rouzaud,[‡] S. Namin,[§] A. K. Keshri,[†] J. J. Valdés,[‡] L. Kos,[‡] N. Tsoukias,[§] and A. Agarwal*,[†]

Mechanical and Materials Engineering, Biological Sciences, and Biomedical Engineering, Florida International University, Miami, Florida 33174

ABSTRACT This study proposes the use of carbon nanotubes (CNTs) as reinforcement to enhance the mechanical properties of a polylactide–caprolactone copolymer (PLC) matrix. Biological interaction of PLC–CNT composites with human osteoblast cells is also investigated. Addition of 2 wt % CNT shows very uniform dispersion in the copolymer matrix, whereas 5 wt % CNT shows severe agglomeration and high porosity. PLC–2 wt % CNT composite shows an improvement in the mechanical properties with an increase in the elastic modulus by 100% and tensile strength by 160%, without any adverse effect on the ductility up to 240% elongation. An in vitro biocompatibility study on the composites shows an increase in the viability of human osteoblast cells compared to the PLC matrix, which is attributed to the combined effect of CNT content and surface roughness of the composite films.

KEYWORDS: PLA-PCL copolymer • carbon nanotube • biodegradable scaffold • strengthening • osteoblast • viability

1. INTRODUCTION

The rapid advancement in the field of tissue engineering and regenerative medicine has led to an increased interest in the use of biodegradable polymers as scaffold material. Biodegradable polymers have been used extensively for multiple bone fixation, repair of osteochondral defects, and ligament and tendon reconstruction (1). Poly-lactic acid (PLA) and poly-ε-caprolactone (PCL) are used as scaffold materials for their excellent bioresorbability and biocompatibility. PLA is a crystalline and brittle polymer with high strength and low elongation at break value. It degrades easily at a faster rate through enzymatic or alkali hydrolysis (2). In contrast, PCL is a semicrystalline polymer of elastomeric nature, which is hydrophobic and degrades at a slower rate (3). PCL is therefore a suitable comonomer of PLA for the preparation of a series of copolymers with mechanical properties ranging from elastomeric to rigid. PLA–PCL copolymer (PLC) has good elongation characteristics, which makes it interesting for bioapplications where both elasticity and degradability are required (4). Hence, copolymerization of PLA and PCL provides a controlled way to adjust the degradation rate, suitable for the intended application (2).

It is equally important that the copolymer should possess excellent mechanical properties as the scaffold material. One of the most effective methods of increasing the mechanical properties (elastic modulus and tensile strength) of a polymer is by reinforcing with a second-phase material. Hence, researchers have used different types of second-phase materials for mechanical strengthening of PLA, PCL, and their copolymers (PLC) (5–16). Among all of these, carbon nanotubes (CNT) seem to be the reinforcement with most potential, due to their very high mechanical properties (Young's modulus 0.2–1 TPa, tensile strength 11–63 GPa) (17, 18) and fiberlike structure. A recent study by Usui et al. (19) demonstrated that multiwalled carbon nanotubes (MWCNT) have very good bone-tissue compatibility and help in the bone repair by accelerating its growth. Further, CNTs get closely integrated in the grown bone without toxic effect. All these findings have caused carbon nanotubes to be the suitable second-phase reinforcement for biodegradable polymers in orthopedic scaffold applications.

Researchers have studied the effect of CNT addition on the mechanical strengthening for PLA (20–23) and PCL (24–26). However, there is currently no report available on a PLC copolymer–CNT composite. Biocompatibility of the CNT-reinforced PLC copolymer composite is another very important issue for scaffold application. Zhang et al. (27) reported that the presence of MWCNTs in PLA inhibits fibroblast cell growth due to less attachment of the cells on the composite surface, although they were not able to establish the cause. Another in vitro study showed that osteoblasts grown on PLA–CNT composite exhibit higher viability and metabolic activity, suggesting it to be a favorable environment for the cells (28). The biocompatibility for PLC–CNT composite is yet to be established, as there are no reports available on biostudies of PCL–CNT and PLC–CNT

[†] Mechanical and Materials Engineering.
[‡] Biological Sciences.
[§] Biomedical Engineering.
Received for review June 19, 2009 and accepted October 4, 2009
DOI: 10.1021/am900423q

Published on Web 10/20/2009

composites. Considering the present scenario, the aim of this study is to explore the effect of multiwalled CNT addition to PLC copolymer on (i) its mechanical properties and (ii) in vitro biocompatibility with human osteoblast cells.

2. EXPERIMENTAL DETAILS

2.1. Synthesis of Composite. Multiwalled CNTs, with an outer diameter of 40−70 nm and length of 1−5 μm, were purchased from Nanostructured & Amorphous Materials, Inc. Houston, TX. The copolymer of L-lactide and ε-caprolactone (PLC), in a molar ratio of 70:30, respectively, was received from Purac Biomaterials, Lincolnshire, IL. For fabricating the composite films, 1 g of PLC was mixed with 20 mL of acetone to form a solution by constant stirring at ~313 K. CNTs were dispersed in acetone by ultrasonicating for 1 h and then mixed with PLC−acetone solution. Finally, the mixture was ultrasonicated for 15 min and poured in a 55 mm diameter glass Petri dish. The films were cured at room temperature in vacuum for 24 h and peeled off from the glass surface. The compositions used for this study were 100 wt % PLC, PLC−2 wt % CNT and PLC−5 wt % CNT, which will be referred to hereafter as PLC, PLC−2CNT and PLC−5CNT, respectively.

2.2. Microstructural Characterization. An FEI PHENOM scanning electron microscope and a JEOL JSM-633OF field emission scanning electron microscope were used at an operating voltage of 5 kV for microstructural characterization of PLC and PLC−CNT composite films. The surface roughness of the polymer films was measured using a Surface Roughness TR200 instrument from Micro Photonics Inc., Irvine, CA. The density of the films was calculated by the geometrical method.

2.3. Evaluation of Mechanical Properties at Multiple Length Scales. A Hysitron Triboindenter (Minneapolis, MN) with 100 nm Berkovich pyramidal tip was used for the nanoindentation testing to study the nanoscale mechanical properties of PLC, PLC−-2CNT and PLC−5CNT composites. The elastic modulus (E) was calculated from the unloading curve using the Oliver−Pharr method (29). More than 50 indents were made on each composite. The indents were made in different regions situated a few millimeters away from each other. In each region, the indents were made at a distance of 9 μm from each other. The total area covered by the indents was greater than 2592 μm^2.

Tensile samples were made from the freestanding PLC, PLC−2CNT, and PLC−5CNT films. Tensile samples were 25 mm long and 5 mm wide, with a gauge length of 5 mm. These tests were carried using an EnduraTEC ELF3200 series tensile machine with a maximum load of 245 N and a maximum crosshead movement of 12 mm. The tests were carried out at a crosshead speed of 6 mm/min. Extensometer was not used for strain measurement, as the tensile samples were small and very lightweight. Tensile sample preparation and tests were carried out as per ASTM-D3039M-08. Three samples from each composition have been tested to get statistical data of the tensile strength for the composite films.

2.4. Biocompatibility Study with Human Osteoblast Cell Line. Human osteoblasts ATCC CRL-11372 (ATCC, Manassas, VA) were cultured for 60 h for cell viability study in a 1:1 mixture of Ham's F12 medium Dulbecco's modified Eagle's medium, with 2.5 mM L-glutamine (Sigma Aldrich, St. Louis, MO). The phenol red free base media was supplemented with 10% fetal bovine serum (Atlanta Biologicals, Lawrenceville, GA) and 100 UI/mL of penicillin and 100 μg/mL of streptomycin (MP Biomedicals, Irvine, CA). Prior to the experiment, PLC composite films (1 cm × 1 cm surface area) were sterilized for 5 h by UV irradiation before being placed into six-well polystyrene Petri dishes (Corning, New York, NY). For cell viability studies, osteoblasts were seeded at a density of 5000 cells per well in 2.5 mL of medium and grown in an incubator at 34 °C with 5% CO_2. After 2.5 days, cells grown on the PLC composite films were stained for 2 min with a phosphate buffer saline 1X solution containing 15 μg/mL of fluorescein diacetate (FDA; MP Biomedicals, Irvine, CA) and 4.5 μg/mL of propidium iodide (PI) (Thermo Fisher Scientific, Waltham, MA) (30) before visualization on a Leica Leitz DM RB fluorescent microscope (Leica, Bannockburn, IL). Digital pictures covering the entire sample area were taken with a Leica DM 500 camera, and live (green) versus dead (red) cells counting was manually performed. "Student t" test was performed to find out the 95% confidence interval for the viability data.

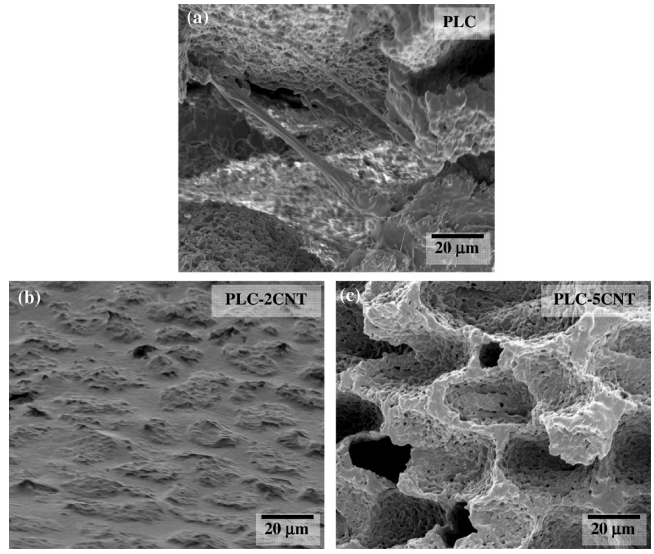

FIGURE 1. SEM micrographs showing cross sections of (a) PLC, (b) PLC−2CNT, and (c) PLC−5CNT composites.

3. RESULTS AND DISCUSSION

3.1. Effect of CNT on the Morphology and Physical Properties of the Composite. PLC, PLC−2CNT and PLC−5CNT composite films show distinct differences in their morphology, porosity, and surface roughness. The density of PLC, PLC−2CNT and PLC−5CNT films is 0.71, 0.90, and 0.69 g/cm^3, respectively. Density results clearly show that PLC−2CNT films have the minimum porosity, which is also confirmed through the SEM images of the cross section of the composite films shown in Figure 1. The difference in porosity is attributed to the behavior of PLC in solution and its interaction with CNTs during curing. PLC makes a colloidal type solution with acetone. During the drying operation, PLC coagulates and forms separated agglomerates. These agglomerates form a porous structure in the PLC film due to shrinkage, which in turn increases the porosity of the composite films. However, in the case of PLC−2CNT film, CNTs are homogeneously dispersed and separated from each other in acetone before addition of PLC. There is no report available on a CNT−PCL/PLC interaction at the interface, although Feng et al. (22) have proven a molecular interaction between PLA and CNT in PLA−CNT composites by appearance of a shift in the Raman spectroscopy peak. The reason for the good bonding could be the helical structure of PLA that tends to form a coil, thus forming a wrap of polymer film on the CNTs. Channuan et

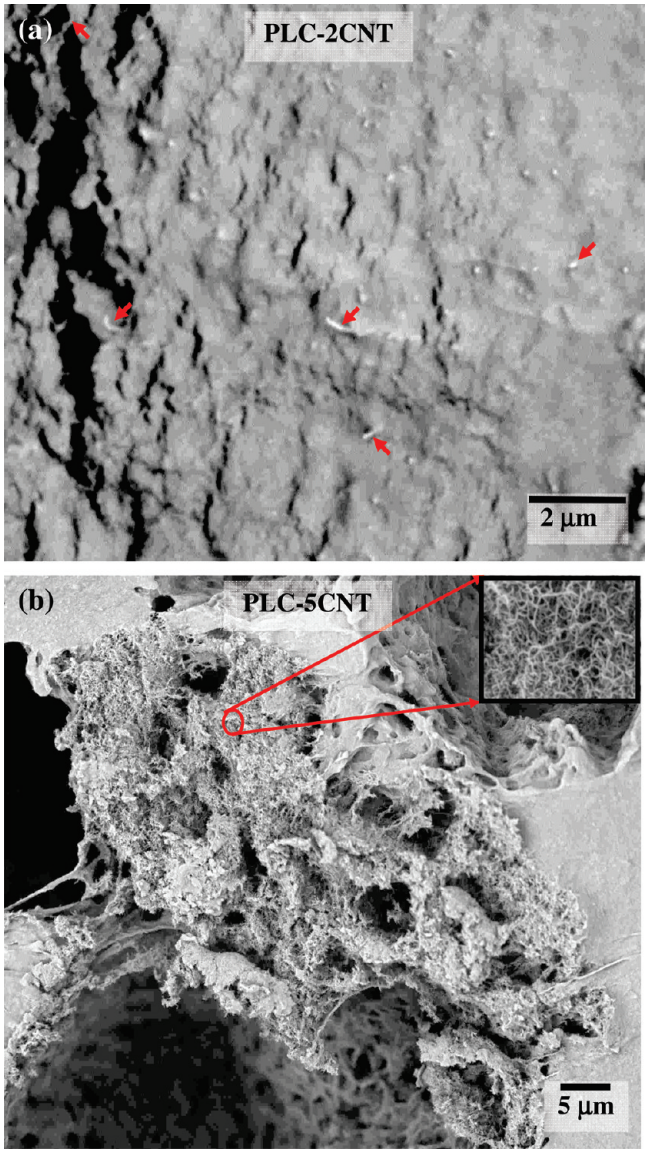

FIGURE 2. SEM micrographs of fracture surfaces of (a) PLC−2CNT with uniformly distributed CNTs (indicated by arrows) and (b) PLC−5CNT, showing agglomerated CNTs. The inset shows agglomerated CNTs at high magnification (24 000×).

al. has shown that a PLA−PCL copolymer retains the helical structure, which is primarily the property of PLA (31). Hence, it can be argued that PLC polymer also retains similar wrapping properties. Thus, uniform distribution of PLC-coated CNTs in solution restricts the PLC coagulation and in turn reduces the porosity in the cured PLC−2CNT film. An SEM image of the cross fracture surface of PLC−2CNT films (Figure 2a) shows very distinctly the uniform distribution of CNTs in the matrix. Further protruded ends of CNTs in the fracture surface indicate good wetting of polymers on the CNT surface.

In contrast, PLC−5CNT composite shows the presence of CNT agglomerates in the matrix and large pores in the vicinity (Figure 2b). A high-magnification SEM image of the CNT agglomerate, presented as an inset in Figure 2b, shows that CNTs present inside the cluster are not wetted by the PLC and thus do not contribute toward effective reinforcement. In the case of PLC−5CNT film, CNTs start agglomerating due to their higher concentration in the solution, which makes them close enough to each other to be dominated by high surface tension. CNTs are no longer in uniform distribution in the suspension; rather, they form agglomerates separated from each other when PLC is added. As a result, the interface area between CNT and polymer is decreased in case of PLC−5CNT composite, as PLC cannot penetrate thoroughly in the CNT agglomerate to wet each CNT separately. Thus, the wetting chemistry being the same for both PLC−2CNT and PLC−5CNT composites, due to differences in the CNT distribution nature, PLC−5CNT shows poor wetting of CNTs by PLC. Hence, a PLC−5CNT composite film forms a porous structure during curing.

3.2. Mechanical Properties of Composite. One of the main aims of synthesizing PLC−CNT composites was to mechanically strengthen biodegradable copolymer for orthopedic scaffold applications. Hence, the characterization of mechanical properties is very important to explore the effectiveness of CNT reinforcement. The elastic modulus (E) of the composite films has been measured at the nanoscale using the nanoindentation technique, whereas the tensile strength has been determined at the macroscale through uniaxial tensile testing. E values were not calculated from the tensile test, as no extensometer was used to measure the strain accurately.

3.2.1. Elastic Modulus by Nanoindentation Technique. Figure 3a shows the typical load vs indentation depth curve for all three compositions obtained through nanoindentation. It could be noticed that, during unloading, the indentation depth for all three samples was fully recovered, indicating the fully elastic behavior of PLC even with the addition of CNTs up to 5 wt %. The lower indentation depth with the higher peak load achieved for PLC−CNT composites is due to the strengthening achieved through CNT reinforcement that resists the elastic deformation of the composites. The increase in the elastic modulus of the PLC with CNT content is due to the reinforcement effect of stiff CNTs. PLC−2CNT composite has an average E value of 160 ± 30 MPa, which is a 100% improvement over PLC (E = 80 ± 30 MPa). PLC−5CNT also shows an improvement of 137% in the E value (190 ± 60 MPa) as compared to the PLC matrix. The average E value of PLC−5CNT is slightly higher than that of PLC−2CNT, which could be due to the localized higher concentration of CNTs and mechanical properties assessed at those spots. E values measured by the nanoindentation technique do not account for the macroscale properties of the composites, such as porosity. This is because the indents were not made on micrometer-sized porous areas of the composite. The improvement in PLC−5CNT composite is minimal, despite higher CNT content due to the clustering of reinforcement. Also, the larger standard deviation in E value of PLC−5CNT composite indicates a lack of homogeneous behavior with 5 wt % CNT addition.

The overall effective elastic modulus of the PLC−CNT composites has also been computed using micromechanics models: viz. the Eshelby approach (32) and Mori−Tanaka

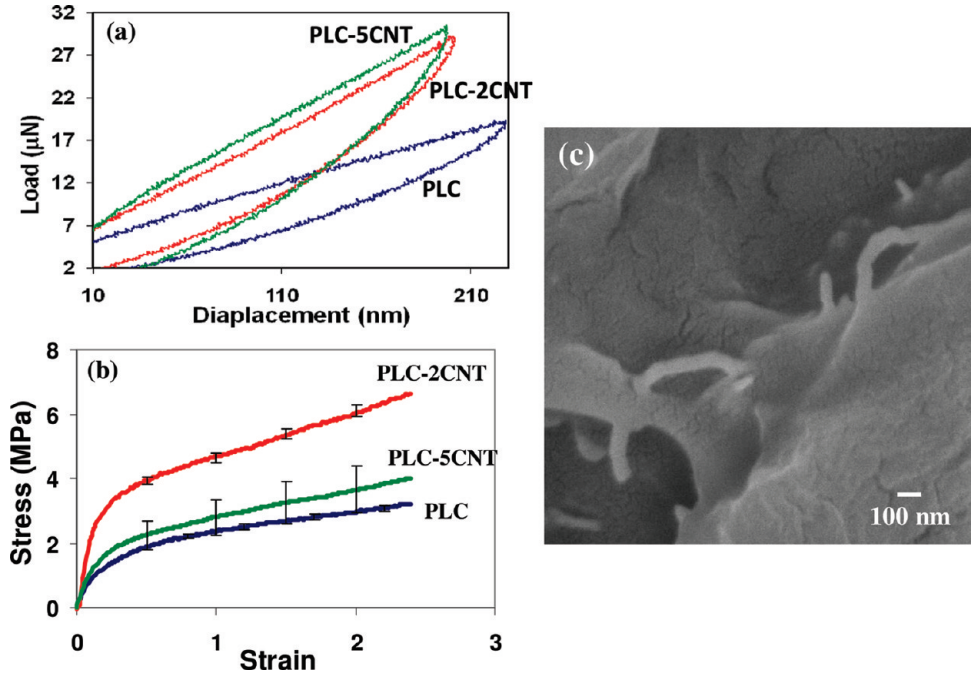

FIGURE 3. Mechanical behavior of PLC, PLC−2CNT, and PLC−5CNT films: (a) representative load−displacement curve for an indent from each composite; (b) stress−strain behavior of three composite films obtained from uniaxial tensile testing; (c) fracture surface of PLC−2CNT composite showing CNT bridging and pullouts.

Table 1. Elastic Modulus of PLC−CNT Composite Obtained by the Nanoindentation Technique and Computed using Micromechanics Models

	E (MPa)		
sample	measured (nanoindentation)	computed (Eshelby)	computed (Mori−Tanaka)
PLC	80 ± 30	80	80
PLC−2CNT	160 ± 30	210	196
PLC−5CNT	190 ± 60	227	192

approach (33). A comparison of the computed (micromechanics models) and measured (nanoindentation) values of the elastic modulus of the composite is given in Table 1. The *E* values calculated by Eshelby and Mori−Tanaka models closely match with the experimentally measured values. The little mismatch between the calculated and measured values could be due to several reasons. The models discussed here have been mainly developed for metal or ceramic matrix composites and assume linear elasticity of the matrix, whereas PLC, being a polymer, may show some viscoelastic nature. Also, the reinforcement for both models is assumed as the ellipsoidal shape, whereas CNTs have the tubular shape.

3.2.2. Tensile Strength by Uniaxial Tensile Test. Stress vs strain curves for all the compositions are shown in Figure 3b. The error bar shows the standard deviation for different samples of the same composition. Average tensile strengths of PLC−2CNT and PLC−5CNT composites are 5.79 and 2.85 MPa, respectively, in comparison to 2.68 MPa for PLC. All the tensile strengths are reported at 240% elongation, which is the limit for the tensile testing machine used in these experiments. Even with 240% elongation, there was no fracture or crack generated in any of the samples and they retrieved the shape upon unloading. Such behavior shows that there is no adverse effect on ductility at least up to 240% elongation, with addition of up to 5 wt % CNT to PLC.

Increase in the tensile strength by 160% through 2 wt % addition of CNT in a PLC matrix can be explained in terms of homogeneous distribution and strong interfacial bonding of CNTs with the matrix that helps in effective load transfer. Fibrous shape and extremely high mechanical properties of CNTs provide the advantages of short fiber strengthening. CNTs help in increasing the fracture strength by bridging the fracture cracks, as evidenced by the presence of CNT bridges and pullouts observed in the fracture surface of PLC−2CNT composite (Figure 3c). On the other hand, PLC−5CNT shows marginal improvement in the tensile strength (6% over PLC), which has been caused by agglomeration of CNTs and pore formation in the matrix as described in section 3.1. The larger error bar in the tensile test behavior in case of PLC−5CNT highlights the heterogeneous behavior of this material at the macroscale (Figure 3c). The effect of agglomeration vs uniform dispersion of fiber reinforcements on the strengthening mechanism could be explained using the shear lag model, which is well accepted for polymer−CNT composites (34). According to the shear lag model, the strength of fiber-reinforced composite depends on the aspect ratio of the reinforcement and shear strength of the fiber−matrix interface (35). The critical fiber length for reinforcement l_c in the shear lag model is described as

$$l_c = \frac{\sigma_f}{2\tau_i} d_f \qquad (1)$$

where σ_f is the ultimate fiber strength, d_f is the fiber diameter, and τ_i is the shear strength at the fiber−matrix

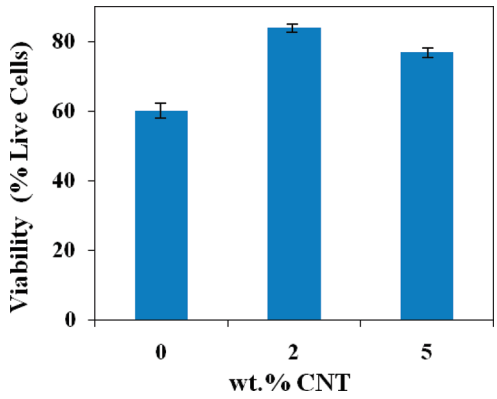

FIGURE 4. Osteoblast cell viability (percent live cells) after 2.5 days of culture on PLC, PLC−2CNT, and PLC−5CNT composite films (*p* value <0.05).

interface or matrix adjacent to the interface, whichever is less. CNTs used in this study have a large aspect ratio (∼15−125). Hence, the fiber length l_f will always be greater than l_c. In this case, the tensile strength will be expressed as

$$\sigma_c = (\sigma_f - \sigma_m)V_f + \sigma_m \quad (2)$$

where σ_m is the matrix strength and V_f is the volume fraction of fiber in the composite. The tensile strength for CNTs being very high (11−63 GPa for MWCNTs), they will serve as very effective reinforcement for enhancement of mechanical properties in a PLC−CNT composite if the interfacial bonding is good (18, 35). The uniform dispersion of CNTs in the matrix helps in ensuring the effective large aspect ratio of the fiber and good interfacial bonding due to polymer wrapping on the surface of individual CNTs, thus providing improvement in mechanical properties. In contrast, agglomeration of CNTs causes a decrease in both the interfacial shear strength and effective aspect ratio of the reinforcement, resulting in insignificant improvement in the mechanical properties of the composite. Thus, PLC−2CNT with well-dispersed CNTs in the matrix shows better tensile strength than PLC−5CNT with poor dispersion and agglomeration of CNTs, though the CNT content is higher.

The literature has shown an increase in *E* value up to 164% with 1.2 wt % CNT addition and 23% improvement in the tensile strength with 0.5 wt % CNT addition in PCL (25, 26, 36). For PLA, up to a 52 wt % increase in *E* by 3 wt % CNT addition and 69% improvement in tensile strength with 2 wt % CNT has been reported (22, 37, 38). The improvement in *E* and tensile strength in a PLA−PCL (70:30) copolymer with 2 wt % CNT addition presented in this study is comparable to the published data on PLA−CNT and PCL−CNT composites. Since there is no available literature on the mechanical behavior of a PLC−copolymer−CNT composite, the results of the present study have been compared to PLA−CNT and PCL−CNT systems.

3.3. Biocompatibility and Viability for Human Osteoblast Cells with PLC−CNT Composites. Biocompatibility of PLC−CNT composites in terms of cell viability has been studied using human osteoblasts. Viability is defined as the ratio of living and dead cells (Figure 4). Fluorescence microscopy images after 2.5 days of growth (Figure 5) show a typical lens shape characteristic of osteoblasts, suggesting the presence of normal cells on PLC, PLC−2CNT, and PLC−5CNT composite films with no significant difference in cellular morphology between the three composites. However, viability data obtained through counting the live to dead cell ratio using fluorescence staining with FDA and PI indicate a significantly higher value of 85% ± 2 live cells in PLC−2CNT film compared to 78% ± 3 and 59% ± 4, respectively, for PLC−5CNT and PLC films (p value <0.05) (Figure 4). The fluorescent images in Figure 5 also provide a comparative picture of the population of cells on the three films. The images show the maximum density of cells in PLC−2CNT, followed by PLC−5CNT and PLC films. The growth behavior of osteoblast cells and their viability on composite films is attributed to (i) the surface roughness of the composite and (ii) the presence of CNTs. The significance of both is discussed in the following paragraphs.

3.3.1. Effect of Surface Roughness on Osteoblast Viability. The surface roughness values for PLC, PLC−2CNT, and PLC−5CNT films are 3.4 ± 0.3, 1.3 ± 0.3, and 3.1 ± 0.4 μm, respectively. When the surface roughness varies in micrometer level, it affects the cell growth and attachment adversely. Higher surface roughness obstructs cell proliferation and attachment due to its increased surface tension and reduced contact angle (39), thus reducing the viability of cells. The PLC−2CNT film has the least surface roughness and provides the most favorable conditions for osteoblast viability. PLC and PLC−5CNT samples, having higher roughness than PLC−

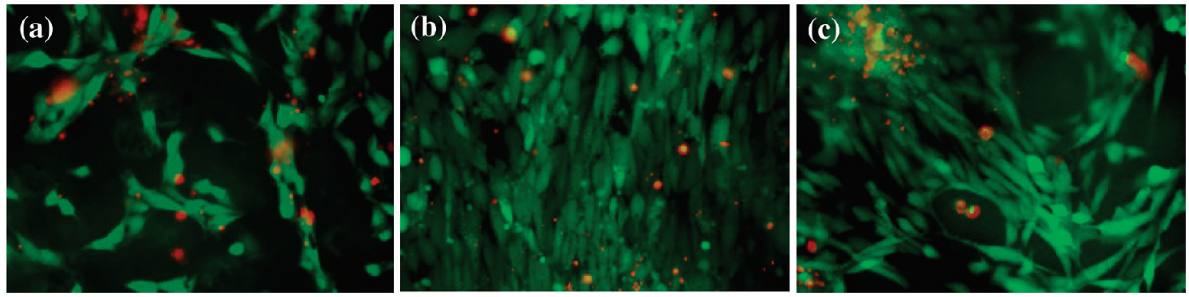

FIGURE 5. Fluorescent images of live (green) and dead (red) osteoblast cells obtained through FDA-PI staining after 2.5 days of growth on (a) PLC, (b) PLC−2CNT, and (c) PLC−5CNT films. All the images are at a magnification of 20X.

2CNT, show poorer viability of osteoblast cells. However, the difference in surface roughness originates from the distribution of CNTs in the matrix and their interaction with the polymer at the solution stage, in the same way as the evolution of porosity as discussed earlier. Hence, the viability difference for surface roughness is also related to the CNT content in the composite films.

3.3.2. Effect of CNT on Osteoblast Viability. It is also observed that PLC−5CNT film shows a significantly higher (78 ± 3%) viability than PLC (59 ± 4%), although the surface roughnesses are similar for both. The processing route being exactly similar for all the composite films, the only difference between PLC and PLC−5CNT is the presence of CNT. Hence, it can be inferred that presence of CNTs plays an active and positive role toward the attachment and proliferation of osteoblast cells. The role of CNTs in promoting osteoblast cell growth on hydroxyapatite−CNT composite surface has already been observed by other researchers (40).

Since PLC is a biodegradable polymer matrix, it may release CNTs into bone and/or the bloodstream over an extended period. Hence, interaction of CNTs with bone and/or blood are also important. The cytotoxicity of CNT is an actively debated issue (41). A recent study implanting MWCNT in a mouse skull (19) has shown that nanotubes get closely integrated in the grown bone without any toxic effect and help in the bone repair by accelerating its growth. Another study on the effect of exposure of CNTs in mice bloodstream (42) revealed that CNTs are not retained by any of the reticuloendothelial system organs (liver or spleen) and are rapidly cleared from the bloodstream through a renal excretion route. Kim et al. (43) studied the interaction of macrophages with CNT−polymer (polycarbonate urethane) and concluded that thepresence of CNTs down-regulates macrophage adhesion and proliferation, resulting in improved orthopedic implant efficacy. Hence, it can be concluded that CNTs have been proven to be noncytotoxic for orthopedic implant applications; in addition, they assist the performance of the same under service conditions.

4. CONCLUSION

CNTs are effective reinforcements, in terms of both mechanical strengthening and biocompatibility, for PLC copolymer in biodegradable scaffold applications. Addition of 2 wt % CNT gives a better dispersion in the PLC matrix, whereas 5 wt % CNT addition leads to their agglomeration, which in turn has an effect on the porosity content of the composite film. An increase in the elastic modulus by 100% and tensile strength by 160% is achieved by 2 wt % CNT addition to the PLC copolymer matrix without any loss in ductility up to 240% elongation. The presence of CNTs in the PLC copolymer matrix promotes osteoblast cell viability.

Acknowledgment. We thank Purac Biomaterials, Lincolnshire, IL, for providing PLC copolymer for research purposes. Mr. George Gomes's assistance during tensile testing and Dr. T. Kim's valuable discussions are also acknowledged. A.A. acknowledges funding from a National Science Foundation CAREER Award (No. NSF-DMI-0547178) and the Office of Naval Research-DURIP program (No. N00014-06-0675).

REFERENCES AND NOTES

(1) Athanasiou, K. *Proceedings of the 1996 Southern Biomedical Engineering Conference*; IEEE: Dayton, OH, March, 1996; pp 541−544.
(2) Zhang, J.; Xu, J.; Wang, H.; Jin, W.; Li, *J. Mater. Sci. Eng. C* **2008**, *29*, 889–893.
(3) Lee, B. T.; Quang, D. V.; Youn, M. H.; Song, H. Y. *J. Mater. Sci.: Mater. Med* **2008**, *19*, 2223–2229.
(4) Karajaleinen, T.; Hiljanen-Vainio, M.; Malin, M.; Seppala, J. *J. Appl. Polym. Sci.* **1996**, *59*, 1299–1304.
(5) Ural, E.; Kesenci, K.; Fambri, L.; Migliaresi, C.; Piskin, E. *Biomaterials* **2000**, *21*, 2147–2154.
(6) Kim, H. W. *J. Biomed. Mater. Res.* **2007**, *83A*, 169–177.
(7) Cerrai, P.; Guerra, G. D.; Tricoli, M.; Krajewski, A.; Guicciardi, S.; Ravaglioli, A.; Maltinti, S.; Masetti, G. *J. Mater. Sci.: Mater. Med.* **1999**, *10*, 283–289.
(8) Russias, J.; Saiz, E.; Nalla, R. K.; Gryn, K.; Ritchie, R. O.; Tomsia, A. P. *Mater. Sci. Eng., C* **2006**, *26*, 1289–1295.
(9) Yang, A.; Wu, R. *J. Mater. Sci. Lett.* **2001**, *20*, 977–979.
(10) Chung, T. W.; Wang, S. S.; Wang, Y. Z.; Hsieh, C. H.; Fu, E. *J. Mater. Sci.: Mater. Med.* **2009**, *20*, 397–404.
(11) Yu, J.; Ai, F.; Dufresne, A.; Gao, S.; Huang, J.; Chang, P. R. *Macromol. Mater. Eng.* **2008**, *293*, 763–770.
(12) Mathew, A. P.; Oksman, K.; Sain, M. *J. Appl. Polym. Sci.* **2005**, *97*, 2014–2025.
(13) Avella, M.; Bogoeva-Gaceva, G.; Buzărovska, A.; Emanuela Errico, M.; Gentile, G.; Grozdanov, A. *J. Appl. Polym. Sci.* **2008**, *108*, 3542–3551.
(14) Li, W.; Qiao, X.; Sun, K.; Chen, X. *J. Appl. Polym. Sci.* **2008**, *110*, 134–139.
(15) Cheung, H. Y.; Lau, K. T.; Tao, X. M.; Hui, D. *Composite B* **2008**, *39*, 1026–1033.
(16) McCullen, S. D.; Stano, K. L.; Stevens, D. R.; Roberts, W. A.; Monteiro-Riviere, N. A.; Clarke, L. I.; Gorga, R. E. *J. Appl. Polym. Sci.* **2007**, *105* (3), 1668–1678.
(17) Singh, S.; Pei, Y.; Miller, R.; Sundarrajan, P. R. *Adv. Func. Mater.* **2003**, *13* (11), 868–872.
(18) Coleman, J. N.; Khan, U.; Blau, W. J.; Gun'ko, Y. K. *Carbon* **2006**, *44*, 1624–1652.
(19) Usui, Y.; Aoki, K.; Narita, N.; Murakami, N.; Nakamura, I.; Nakamura, K.; Ishigaki, N.; Yamazaki, H.; Horiuchi, H.; Taruta, S.; Kato, H.; Ahm Kim, Y.; Endo, M.; Saito, N *Small* **2008**, *4* (2), 240–246.
(20) Wu, D.; Wu, L.; Zhang, M.; Zhao, Y. *Poly. Degrad. Stab.* **2008**, *93*, 1577–1584.
(21) Zhao, Y.; Qiu, Z.; Yang, W. *Compos. Sci. Technol.* **2009**, *69*, 627–632.
(22) Feng, J.; Sui, J.; Cai, W.; Wan, J.; Chakoli, A. N.; Gao, Z. *Mater. Sci. Eng., B* **2008**, *150*, 208–212.
(23) Chen, G. X.; Shimizu, H. *Polymer* **2008**, *49*, 943–951.
(24) Wu, D.; Wu, L.; Sun, Y.; Zhang, M. *J. Polym. Sci. B: Polym. Phys.* **2007**, *45*, 3137–3147.
(25) Kim, H. S.; Chae, Y. S.; Choi, J. H.; Yoon, J. S.; Jin, H. J. *Adv. Compos. Mater.* **2008**, *17* (2), 157–166.
(26) Xu, G.; Du, L.; Wang, H.; Xia, R.; Ming, X.; Zhu, Q. *Polym. Int.* **2008**, *57*, 1052–1066.
(27) Zhang, D.; Kandadai, M. A.; Cech, J.; Roth, S.; Curran, S. A. *J. Phys. Chem. B* **2006**, *110* (26), 12910–12915.
(28) Pow, B. Y. F.; Mak, A. F. T.; Wong, M. S.; Yang, M. *Adv. Mater. Res.* **2008**, *47−50*, 1347–1350.
(29) Oliver, W. C.; Pharr, G. M. *J. Mater. Res.* **1992**, *7* (6), 1564–1583.
(30) Valdes, J. J.; Weeks, O. I. *Brains Res.* **2009**, *1268*, 1–12.
(31) Channuana, W.; Siripitayananona, J.; Molloy, R.; Sriyai, M.; Davisa, F. J.; Mitchell, G. R. *Polymer* **2005**, *46*, 6411–6428.
(32) Eshelby, J. D. *Proc. R. Soc. London, Ser. A* **1957**, *241* (1226), 376–396.
(33) Mori, T.; Tanaka, K. *Acta Mater.* **1973**, *21* (5), 571–574.
(34) Gao, X. L.; Li, K. *Int. J. Sol. Struct.* **2005**, *42*, 1649–1667.
(35) Mallick, P. K. In *Fiber-Reinforced Composites-Materials, Manufacturing and Design*, 2nd ed.; Marcel Dekker: New York, 1993; pp 96−98.

(36) Kim, H. S.; Park, B. H.; Yoon, J. S.; Jin, H *J. Solid State Phenom.* **2007**, *124*−*126*, 1133–1136.
(37) Kim, H. S.; Park, B. Y.; Yoon, J. S.; Jin, H. J. *Eur. Polym. J.* **2007**, *43*, 1729–1735.
(38) Krul, L. P.; Volozhyn, A. I.; Belov, D. A.; Poloiko, N. A.; Artushkevich, A. S.; Zhdanok, S. A.; Solntsev, A. P.; Krauklis, A. V.; Zhukova, I. A. *Biomol. Eng.* **2007**, *24*, 93–95.
(39) Khosroshahi, M. E.; Mahmoodi, M.; Saeedinasab, H.; *Lasers Med. Sci.* **2008**, DOI 10.1007/s10103-008-0628-1.
(40) Xu, J. L.; Khor, K. A.; Sui, J. J.; Chen, W. N. *Mater. Sci. Eng., C* **2009**, *29*, 44–49.
(41) Fiorito, S. In *Carbon Nanotube: Angels or Demons?*, 1st ed.; Pan Stanford Publishing: Singapore, 2008; ISBN: 9814241016, 9789814241014.
(42) Singh, R.; Pantarotto, D.; Lacerda, L.; Pastorin, G.; Klumpp, C.; Prato, M.; Bianco, A.; Kostarelos, K. *Proc. Natl. Acad. Sci. U.S.A.* **2006**, *103* (9), 33578–3362.
(43) Kim, J. Y.; Khang, D.; Lee, J. E.; Webster, T. J. *J. Biomed. Mater. Res. A* **2009**, *88A* (2), 419–426.

AM900423Q